Integrated Polymer Optoelectronic Time Delay Device for an X-band Phased Array Antenna System

Brie Howley[1*], Xiaolong Wang[1], Yihong Chen[2], & Ray T. Chen[1]

[1]Microelectronics Research Center, The University of Texas at Austin, 10100 Burnet Rd., Bldg 160, Austin, TX 78758

[2]Omega Optics, Austin, TX 78758

ABSTRACT

A 4-bit polymer optoelectronic true time delay device is demonstrated. The device is composed of monolithically integrated, low loss, passive polymer waveguide delay lines and 2x2 polymer thermo-optic switches. Waveguide junction offsets and air trenches simultaneously reduce the bending loss and device area. Simulations are used to optimize the trench and offset structures for fabrication. The 16 time delays generated by the device are measured to range from 0 to 177 ps in 11.8 ps increments. The packaged device has an insertion loss of 14.5 dB and the delay switching speed is 2 ms. The delays generated by the device are suitable for steering a 1D or 2D sub-array of an X-band phased array antenna system.

Keywords: phased-array antenna, optoelectronic, waveguide, polymer, thermo-optic, optical switch

1. INTRODUCTION

Waveguide transmission lines are excellent candidates for the transmission and control of RF signals in wide bandwidth phased array antenna (PAA) systems. Optical waveguides provide low RF and microwave signal propagation loss, immunity to electromagnetic interference and reduced system size and weight. Waveguide optical delay lines, patterned by photolithographic methods, are able to deliver precise delays with sub-picosecond resolution for phased array antenna systems. Additionally, optical delay lines can be integrated with lasers, modulators, switches, and detectors to form compact planar lightwave circuits (PLC's) that are ideal for PAA applications.

Several material systems have been used to fabricate waveguide optical delay lines, notably silica[1], silicon on insulator (SOI)[2], and polymers[3]. In contrast with alternative material systems, polymer waveguides are easier to fabricate on almost any substrate of interest. The thermo-optical coefficient, $\Delta n/\Delta T$, of polymer materials can be in excess of an order of magnitude greater than that of SiO_2, [4] making polymers ideal candidates for low power, thermo-optic switches. Additionally, the refractive indices of polymer waveguide materials can be adjusted across a broad range to form waveguide structures with mode profiles similar to those of single mode silica fiber. Matching the mode profiles enables minimal coupling losses between silica fiber and the polymer waveguide structures.

This paper shows how polymer optical waveguides can by used to build fully integrated true time delay (TTD) devices. Polymer channel waveguides are designed and fabricated to provide low loss optical transmission. Offset and trench structures are introduced as methods to reduce bending loss. These structures are evaluated by beam propagation method (BPM) simulations. Total internal reflection (TIR) thermo-optic switches are designed and fabricated. Results of these switches' performance are presented. The TIR switches are then integrated monolithically with waveguide delay lines and bend loss reduction structures to form a compact 4-bit waveguide delay device. The delay device is then packaged and tested. The generated delays are measured along with the device insertion loss.

* brie@ece.utexas.edu; phone 512-232-2586; fax 512-471-8575

Optoelectronic Integrated Circuits VIII, edited by Louay A. Eldada, El-Hang Lee,
Proc. of SPIE Vol. 6124, 61240Z, (2006) · 0277-786X/06/$15 · doi: 10.1117/12.657962

2. A POLYMER WAVEGUIDE STRUCTURE

The polymer waveguide is the basic building block of the polymer TTD device. The performance of both the delay lines and the waveguide based thermo-optic switches are directly related to the waveguide's properties. It is therefore necessary to engineer high quality optical waveguides with suitable mode characteristics and loss values.

The fabrication process for the polymer waveguides used in the optical switches and delay lines is shown in Fig 1. A polymer bottom cladding material is spin coated onto a clean substrate. The thickness of the layer is determined by the spin speed. After UV and thermal curing, a second layer of polymer is spun which serves as the core layer. This core layer has a slightly higher refractive index which is needed for guiding the light by total internal reflection. A suitable thickness of a hard masking material is then deposited followed by photoresist which is defined by photolithography. The hard mask is then patterned by either a wet or dry etching method depending on the hard mask material. Once the hard mask is properly defined, reactive ion etching (RIE) is used to form the channel waveguides in the core material. The remaining hard mask is then removed and a polymer top cladding layer is spin coated and cured.

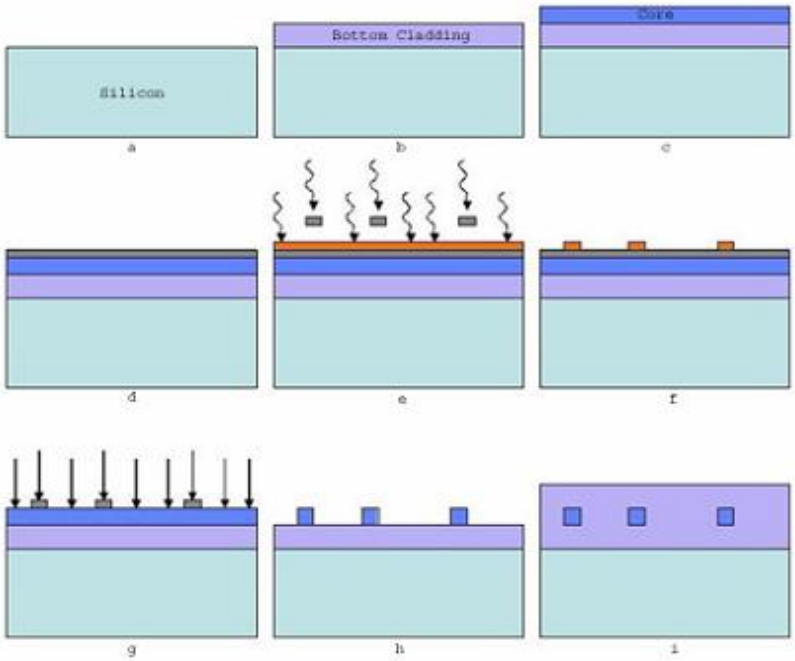

Fig. 1. The polymer waveguide fabrication process.

Fig 2 is an SEM image of the fabricated waveguide core structure which is 6.5 μm tall and 6.5 μm wide. The roughness of the core sidewalls is related to the waveguide propagation loss.[5] It is therefore critical to use a waveguide fabrication procedure that is optimized to result in a core with smooth surfaces and vertical sidewalls. Details of the optimized polymer waveguide fabrication procedure has previously been published.[6]

In order to avoid intermodal dispersion which will lead to inaccurate time delays, it is necessary for the waveguide to allow only fundamental mode propagation. Fig 3a shows beam propagation method (BPM) simulation results for the mode profile of a 6.5 x 6.5 μm channel waveguide. The simulation was performed with a core and cladding refractive index matching those of our polymer materials, 1.46 and 1.45 respectively. Both TE and TM modes showed single mode behavior at the operating wavelength of 1.55 μm. The 1/e mode field diameter (MFD) was calculated to be 7.8 μm. Fig 3b shows a near field image of a fabricated waveguide as a comparison to the simulation results. The

experimentally measured MFD was 7.5 μm. Propagation losses of these straight waveguides were measured to be as low as 0.38 dB/cm at the wavelength of 1.55 μm.

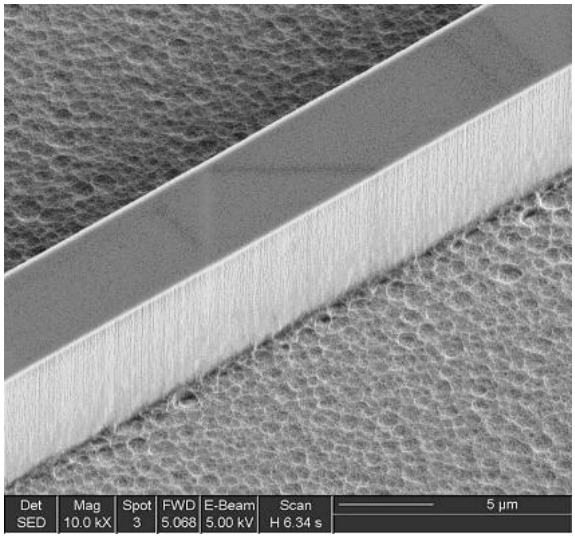

Fig. 2. SEM image of a channel waveguide core.

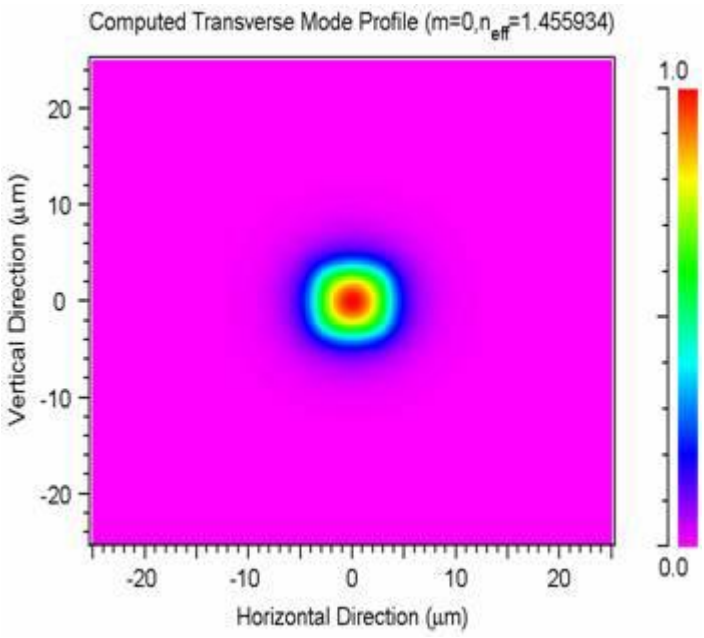

Fig. 3a. BPM simulation of the mode pattern for the polymer channel waveguide with a MFD of 7.8 μm

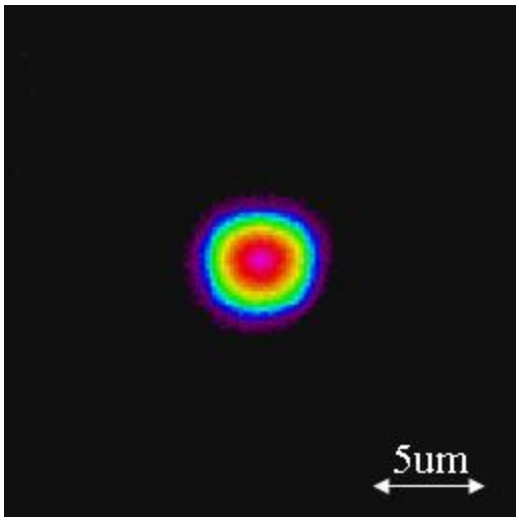

Fig. 3b showing the near field image from the end of the fabricated waveguide with a MFD of 7.5 μm.

3. BEND LOSS REDUCTION STRUCTURES

Low index contrast systems, such as polymers, can provide low fiber to waveguide coupling losses and low propagation losses due to the small refractive index difference between the core and cladding. However, a major drawback of any low index contrast system for a PLC application is the large footprint attributable to the requirement of large waveguide bend radius for low loss.[7] Polymers have the advantage of a widely tunable refractive index[8] but this still leaves a compromise between coupling loss and bend loss. The large bend radii requirement for low index contrast systems is not practical for devices requiring large scale integration such as optical delay lines[9] and is detrimental to the device yield.

Air trenches have been proposed to reduce the radii by increasing the index contrast of a curved waveguide segment.[10-13] By increasing the index contrast within the waveguide bend region, the mode is tightly confined in order to prevent bend radiation losses while the propagation losses are not significantly affected. Another modification to the waveguide design used to decrease bending losses is the offset. Waveguide offsets shift straight waveguide segments laterally with respect to curved waveguides in order to decrease the mode mismatch.[14,15] This in turn minimizes the junction loss between the curved and linear waveguide segments.

Fig 4 illustrates a top view of a channel waveguide junction between straight and curved waveguide segments. The structure utilizes both a trench, which is assumed to be filled with air (n_{Tr}=1), and an offset. The core and cladding indices are n_{Co} and n_{Cl}, respectively, and the waveguide has a bend radius of R. The width of the trench, w_{Tr}, and the separation between the inside radius of the trench and the outside radius of the waveguide core, d, are also labeled. By placing the air trench sufficiently close to the waveguide core, (reducing w_{Tr}) the evanescence tail is reduced and a decreased bend loss should be observed.

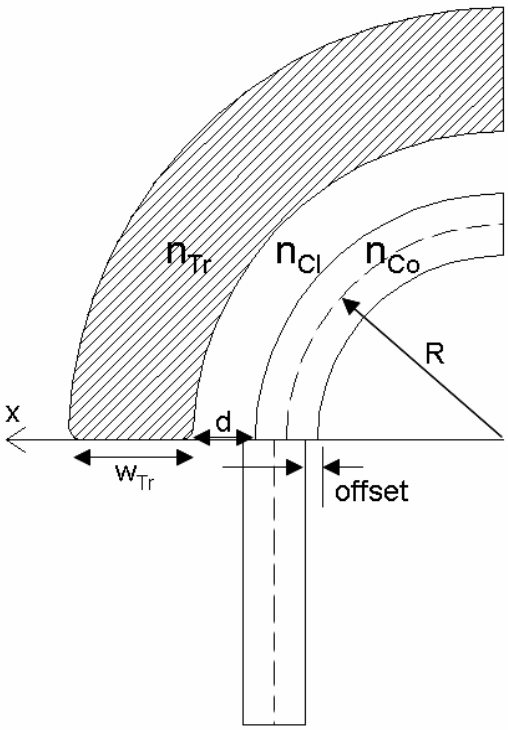

Fig 4. A diagram of the waveguide core using offset and trench (hatched area) structures.

Simulations were performed to evaluate the bend and junction loss versus bend radius of four different cases: (1) standard bends employing neither offsets nor trenches, (2) waveguide junctions employing optimal offsets, (3) waveguides with trench structures, and (4) both optimal offsets and trenches. The 180º bends were simulated with a BPM equivalent index transformation in order to avoid paraxial effects. This method has been shown to be accurate for bends with radii much larger than the core width dimension.[16] Fig 5 shows the results of these simulations. It is seen that without any trench structures the bend loss exhibits an exponential increase as the bend radius is reduced. However, by using trenches and offsets together, the bend radius can be reduced to 1.5 mm without any significant increase in loss.

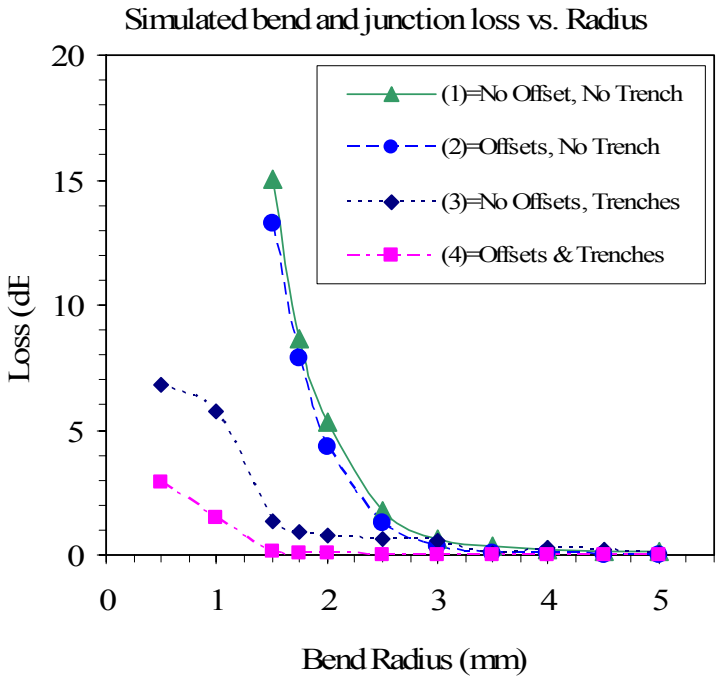

Fig 5. The BPM simulated bend and junction loss for a 180º bend as a function of waveguide bend radius for cases (1)-(4). The trench separation is 7 μm with an operating wavelength of 1.55 μm.

4. POLYMER THERO-OPTIC SWITCHES

The thermo-optic (TO) effect of polymeric materials is negative, i.e., the refractive index of the polymer decreases as the temperature rises. Thus, a TIR optical switch can be formed if a heater is set at the crossing point of a symmetric X junction.[17,18,19] Compared with various TO switch configurations, such as a digital optical switch (DOS)[20], a Mach-Zehnder interferometer (MZI) switch[21], or a directional coupler switch[22], TIR switches have a significant advantage in their broad optical bandwidth (or equivalently, their wavelength insensitivity).

Fig 6 shows the schematic diagram of a 2 x 2 TO TIR switch. Two input waveguides of a suitable pitch are connected to bend waveguides. The bend waveguides have a radius of curvature, R, which is large enough to provide negligible bending loss and guided mode perturbation. The bend waveguides are then connected by two straight waveguides to form an X junction. Horn structures are introduced near the junction area to reduce the cross talk and to make the switch operable with the temperature gradient induced by a thin film heater. The input and output sides of the switch are symmetric. The thin film heater is formed by a layer of gold film deposited above the top polymer cladding layer. For the case of the TO TIR switch described herein, the pitch of the input/output waveguides is 250μm and R is 10mm.

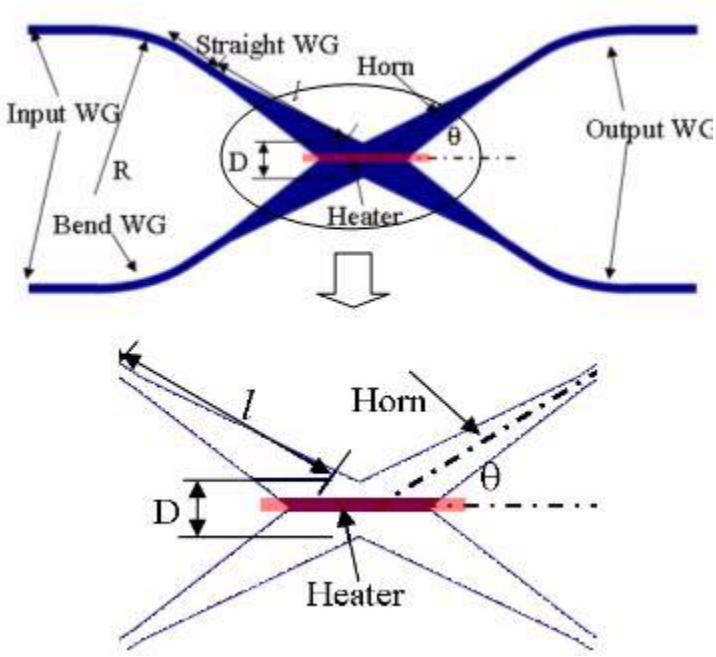

Fig 6. Schematic of the structure of a TIR thermo-optic switch and magnified view of the X-juction with a heater.

The most critical parameters of the switch are the taper length *l*, the junction width *D*, and the half branch angle *θ*. These parameters have been adjusted, through simulation and experimentation, to achieve the desired operating characteristics for the delay device. For the results reported, the values of *l, D,* and *θ* are 1442 μm, 50 μm, and 4°, respectively. Fig 7 shows a top down optical microscope picture of the X-junction region of a fabricated 2x2 TO TIR switch. With a total device length of 19mm, the lowest insertion loss we have achieved is 2.8dB.

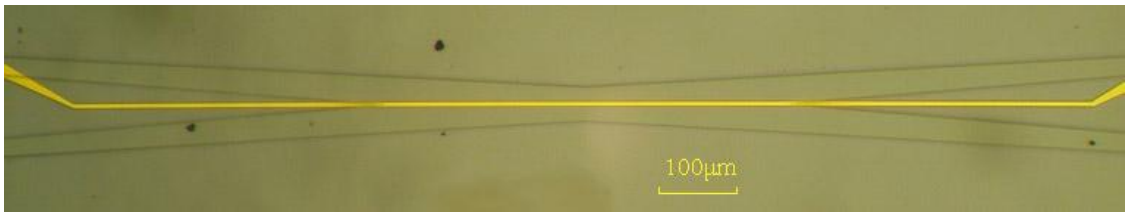

Fig 7. Optical microscope picture of the X-junction region of a fabricated 2x2 TO TIR switch.

Fig 8 shows the optical power in the bar and cross ports as a response to the electrical drive power supplied to the thin film heater. The tested switch has a cross talk of -31dB in the cross state and a power consumption of 0mW. The zero static power consumption is a profitable feature since it can reduce the average driving power in real applications. With a driving power increase, the optical power in the cross port will decrease while the optical power in the bar port increases. Eventually, the switch will reach the bar state. The bar state power consumption is defined as the driving power resulting in maximum optical power in the bar port, which is 44mW while the bar state cross talk is -32dB.

The switching time of the TIR switch is determined by the thermal conductivity and thickness of the polymer. The total polymer thickness is approximately 20μm. A 200Hz square waveform with an amplitude of 1.3V and an offset of 0.65V

was used to drive the heater of the switch. The optical response in the two output channels, as shown in Fig 9, demonstrates a delay of 1.5ms for t_{rise} and 2ms for t_{fall}.

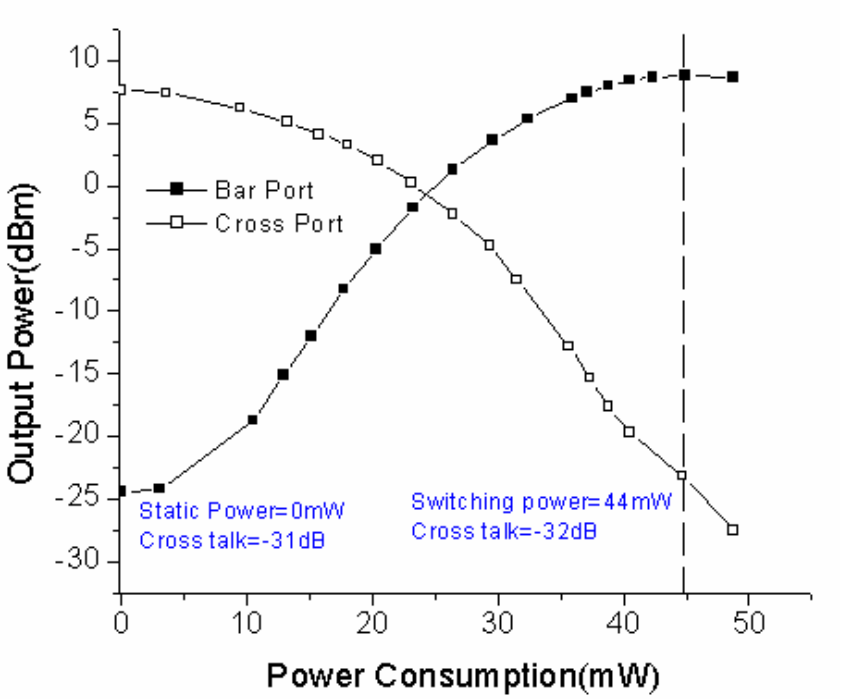

Fig 8. Optical power response to the electrical drive power.

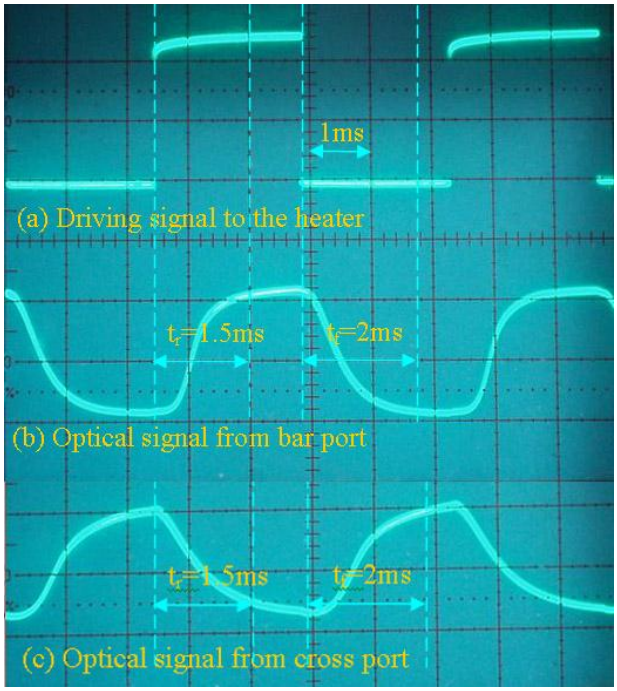

Fig 9. Time response of the TO TIR switch.

5. A FULLY INTEGRATED TRUE TIME DELAY DEVICE

The configuration of the designed TTD module is shown as Fig 10, which consists of input/output waveguides, five 2×2 TO TIR switches, four reference lines and four delay lines. Due to the fully-integrated approach, both optical switches and waveguide delay lines have a core index of 1.46 and a cladding index of 1.45. The 6.5μm×6.5μm waveguide core cross section constrains the waveguide to be single mode and provides a good coupling efficiency with a single mode fiber. The TIR switches have a 250μm waveguide pitch and 4° half branch angle. The switch waveguides are tapered from 6.5μm to 48μm in the junction area to reduce the switch cross talk. The switches are 4924μm in length including 500μm straight waveguide segments on each side to stabilize the optical mode into/out of the delay lines. Thin film heaters for the switches are placed on the top cladding layer and connected to bonding pads through lead lines.

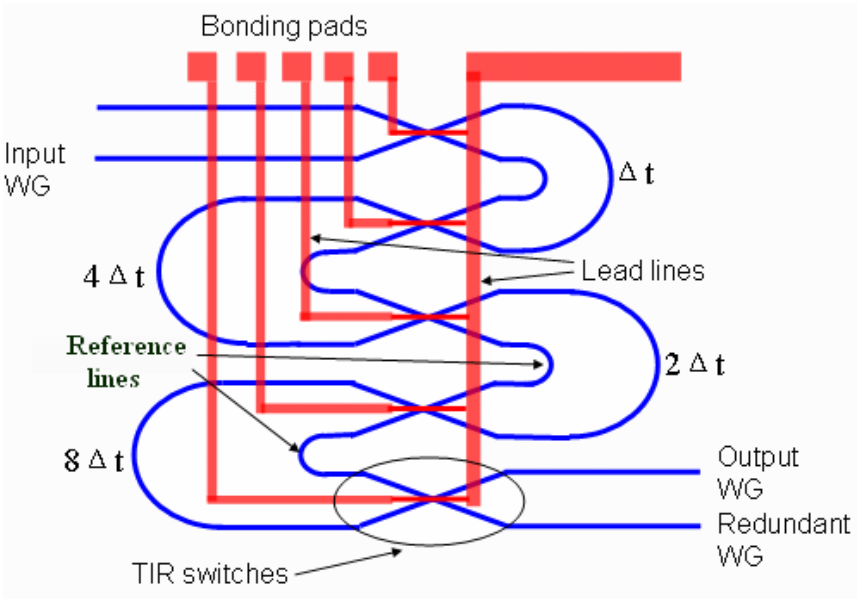

Fig 10. Schematic of the 4-bit TTD device.

Optimized waveguide offsets and trench structures are implemented in the waveguide bends in order to simultaneously reduce the device size and decrease the device insertion loss. The bend radii of the reference lines are 1.5 mm, and those of the delay lines are 1.75mm. 1.3 and 1.5 μm lateral offsets are used for the delay and reference waveguide bends, respectively. A 20 μm wide air trench is used in the bend regions in order to confine the mode and prevent excess bend loss. The separation between the waveguide core and trench is 7 μm. Fig 11 shows an SEM cross section of a polymer waveguide bend with a trench. The approximate location of the waveguide core is represented by the square. Fig 12 shows an optical microscope top down view of the junction between straight and curved waveguide segments where both the trench and offset are visible.

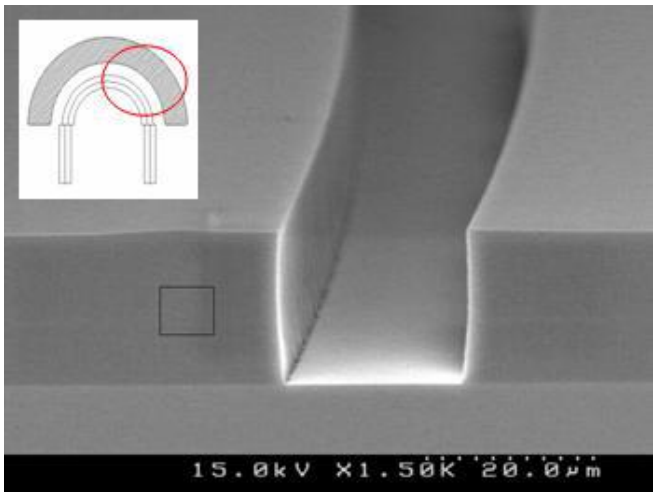

Fig 11. SEM cross-sectional image of the trench structure. Approximate location of the waveguide core is indicated by the square to the left of the trench.

Fig 12. Top view of a waveguide junction employing both a trench and an offset.

The TTD device was fabricated on a silicon wafer substrate. The wafer was then diced and the end faces of the device chip were polished in order to enable efficient coupling. The device size was 1.5 x 2.1 cm. Single mode optical fiber pigtails were epoxied to the device's input and output waveguides. The optical assembly was then attached to a PCB and gold wire bonds were used to make electrical connections to the TO TIR switches. The fiber in/fiber out insertion loss of the packaged TTD device was 14.5 dB which is in close agreement with the theoretical lowest insertion loss of 13.9 dB.

Delay values generated by the 4-bit TTD device were measured. A continuous-wave laser, operating at 1.55 μm, was modulated by a LiNbO modulator fed by an HP8510C network analyzer. The output of the modulator was input to the delay device. A 45 Ghz bandwidth photodetector was used to convert the modulated optical signal to an electrical signal that was fed back to the network analyzer. Fig 13 shows the measured microwave phase versus frequency response from 200 Mhz to 12 Ghz. The shortest delay path, 0Δt, served as the reference value. The incremental delay value, Δt, was designed to be 11.8 ps. The time delays for each delay path were calculated from the slope of the fitted lines and are also shown in Fig 13. All measured delay values have less than 0.25 ps error from the designed delays. This measurement error is due to jitter in the network analyzer's measurement of the phase.

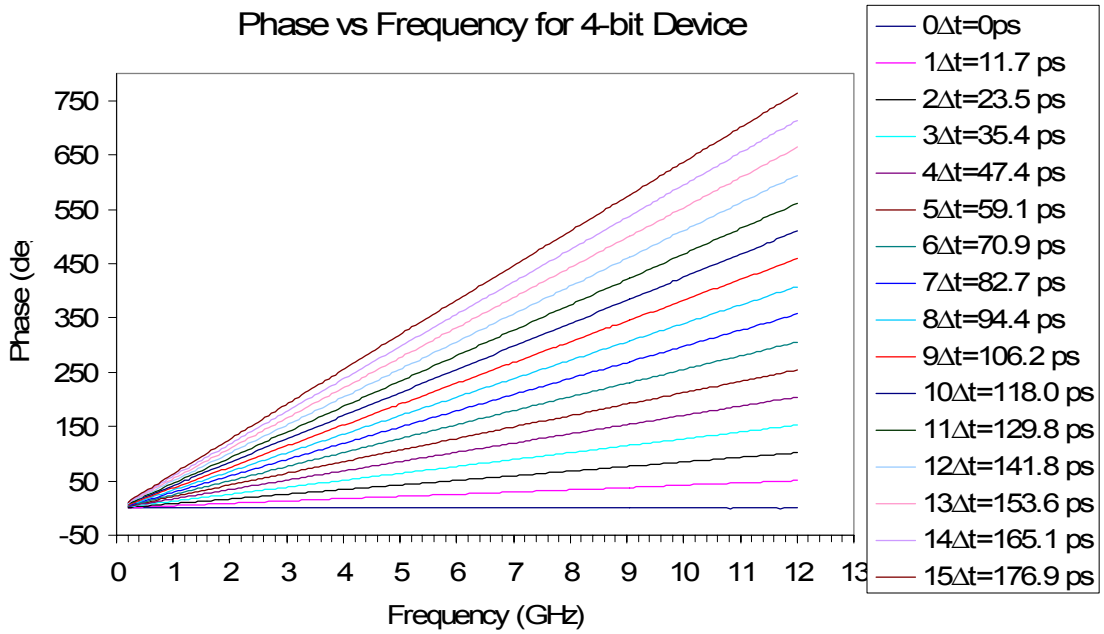

Fig 13. Phase versus RF frequency measurement results for each of the sixteen delay states.

The highly linear phase versus frequency response is indicative of true time delay. The delays generated by this device are capable of providing a full ±45º of steering for a PAA sub array operating from 8-12 Ghz. Larger steering angles or larger arrays are possible with higher frequency antenna systems.

6. CONCLUSION

Polymer waveguides were used to construct optical delay lines and 2x2 TO TIR switches. 20 μm wide air trenches were used to confine the mode in the waveguide bends in order to prevent bending loss. Lateral waveguide offsets of 1.3 and 1.5 μm were used to reduce the waveguide junction loss between straight and curved waveguide bends. Polymer waveguide bends with radii of curvature as small as 1.5 mm had negligible bend loss due to these bend loss reduction techniques. 2x2 thermo-optic switches based on an X-junction TIR effect were designed and fabricated. The switches had an insertion loss of 2.8 dB, a crosstalk of less than -31 dB, bar state power consumption of 44 mW, and a response time of 2 ms. A fully integrated polymer waveguide TTD device was fabricated using these switches and waveguide structures. The TTD device was capable of generating delays for an X-band PAA subarray. The insertion loss and device size were both significantly reduced by the use of the bend loss reduction structures.

REFERENCES

1. K. Horikawa, I. Ogawa, T. Kitoh, H. Ogawa, "Photonic Integrated Beam Forming and Steering Network Using Switched True-Time-Delay Silica-Based Waveguide Circuits", *IEICE Trans. Electron*, E79-C, pg. 74-79, 1996

2. S. Yegnanarayanan, P.D. Trinh, F. Coppinger, B. Jalali, "Compact Silicon-Based Integrated Optic Time Delays", Phot. Tech. Lett., **9**, pg. 634-635, 1997

3. S. Tang, B. Lin, N. Jiang, D. An, Z. Fu, L. Wu, R.T. Chen, "Ultra-low-loss Polymeric Waveguide Circuits for Optical True-time delays in Wideband Phased Array Antennas," Opt. Eng., **39**, pg. 643-651, 2000

4. L. Eldada, "Optical Communication Components", Rev. Sci. Instrum., **75**, pg. 575-593, 2004

5. K.K. Lee, D.R. Lim, L.C. Kimerling, J. Shin, F. Cerrina, "Fabrication of ultralow-loss Si/SiO_2 waveguides by roughness reduction", Opt. Lett., **26**, pg. 1888-1890, 2001

6. B. Howley, X. Wang, Q. Zhou, Y. Chen, R.T. Chen, "Polymer Waveguides and Thermo-Optic Switches for an Optical True Time Delay Phased Array Antenna," *Proceedings of SPIE*, Vol. 5731, 2005

7. F. Ladouceur, J.D. Love, *Silica-based Buried Channel Waveguides and Devices*, Ch. 10, Chapman & Hall, London, 1996

8. L. Eldada, "Advances in telecom and datacom optical components", Opt. Eng., **40**, pg.1165-1178, 2001

9. B. Howley, Y. Chen, X. Wang, Q. Zhou, R.T. Chen, "2-bit Reconfigurable True Time Delay Lines Using 2x2 Polymer Waveguide Switches", Phot. Tech. Lett., **17**, pg.1944-1946, 2005

10. J. Yamauchi, M. Ikegaya, H. Nakano, "Bend Loss of Step-Index Slab Waveguides with a Trench Section", Microwave and Opt. Tech. Lett., **5**, pg. 251-254, 1992

11. C. Seo, J.C. Chen, "Low Transition Losses in Bent Rib Waveguides", J. Lightwave Tech., **14**, pg. 2255-2259, 1996

12. M. Rajarajan, S.S.A. Obayya, B.M.A. Rahman, K.T.V. Grattan, H.A. El-Mikati, "Design of compact optical bends with a trench by use of finite-element and beam-propagation methods", App. Opt., **39**, pg. 4946-4953, 2000

13. M. Popovic, K. Wada, S. Akiyama, H.A. Haus, J. Michel, "Air Trenches for Sharp Silica Waveguide Bends", J. Lightwave Tech., **20**, pg. 1762-1772, 2002

14. T. Kitoh, N. Takato, M. Yasu, M. Kawachi, "Bending Loss Reduction in Silica-Based Waveguides by Using Lateral Offsets", J. Lightwave Tech., **13**, pg. 555-562, 1995

15. S. Tomljenovic-Hanic, J.D. Love, A. Ankiewicz, "Low-loss singlemode waveguide and fibre bends", Elect. Lett., **38**, pg. 220-222, 2002

16. L. Lerner, "Minimum Bending Loss Interconnection for Integrated Optics Waveguides", Elect. Lett., **29**, pg. 733-735, 1993

17. C.S Tsai, B.Kim and F.R. Akkari, "Optical channel waveguide switch and coupler using total internal reflection," J. of Quanum. Electron., **14**, pg. 513-517, 1978

18. J.Yang, Q.Zhou and R.T.Chen, “Polyimide -waveguide-based optical switch using total-internal – reflection effect,” Appl. Phys. Lett., **81**, pg. 2947-2949, 2002

19. X. Wang, B. Howley, M. Chen, et al, “Polymer Based Thermo-optic Switch for Optical True Time Delay,” *Proceedings of SPIE,* Vol. 5728**,** pg. 60-67, 2005

20. Y.Silberberg, P.Perimutter and J.E.Baran, “Digital Optical Switch,” Appl. Phys. Lett*.,* **51**, pg.1230-1232, 1987

21. Q. Lai, , W. Hunziker, H. Melchior, “Low-power compact 2×2 thermooptic silica-on-silicon waveguide switch with fast response,” Phot. Tech. Lett., **10**, pg.681-683 ,1998

22. H. Kogelnik and R.V.Schmidt, “Switched directional couplers with alternating Δβ,” J. Quantum Electron., **12**, pg.396-401, 1976